Supplementary Information

CO_2 adsorption-enhanced semiconductor/metal-complex hybrid photoelectrocatalytic interface for efficient formate production

Xiaofeng Huang,[a] Qi Shen,[a] Jibo Liu,[a] Nianjun Yang*[b] and Guohua Zhao*[a]

[a] School of Chemical Science and Engineering, Tongji University, 200092 Shanghai, China

[b] Institute of Materials Engineering, University of Siegen, 57076 Siegen, Germany

*Corresponding Author. Tel: +86-21-65981180; Fax: +86-21-65982287

*Corresponding Author. Tel: +49-271-7402531; Fax: +49-271-7402442

E-mail address: g.zhao@tongji.edu.cn

E-mail address: nianjun.yang@uni-siegen.de

Table of content

1. Experimental Section

1.1 Chemicals and Solutions

Cobalt nitrate hexahydrate [$Co(NO_3)_2 \cdot 6H_2O$], ruthenium trichloride hydrate ($RuCl_3 \cdot xH_2O$), ammonium fluoride (NH_4F), hexamethylenetetramine (HMT), 2,2'-bipyridine(bpy), 1,10-phenathroline, 2,3,4,5,6-pentafluorobenzyl bromide, tetrabutylammonium hexafluorophosphate ($TBAPF_6$), sodium tetrafluoroborate ($NaBF_4$), ferric nitrate nonahydrate [$Fe(NO_3)_3 \cdot 9H_2O$], potassium bromide (KBr), formaldehyde, resorcinol, sodium carbonate, pyrrole, lithium chloride , dimethyl sulphoxide (DMSO), and acetonitrile were purchased from Sinopharm Chemical Reagent Co., Ltd. (SCRC, China). They were analytical grade reagents and used without further purification. D_2O was purchased from Cambridge Isotopic Laboratory (D enrichment: 99.9%). $NaH^{13}CO_3$ was purchased from Sigma-Aldrich (^{13}C enrichment: 98%). $^{13}CO_2$ and $H^{13}COONa$ (^{13}C enrichment: 98%) were purchased from Shanghai Engineering Research Center of Stable Isotope. 2% Nafion-117 solution was bought from Alpha-Aesar. Fluorine-doped tin oxide coated glass (FTO, 14 Ω sq^{-1}) was purchased from Nippon Sheet Glass Group (Japan). 0.1 M Na_2SO_4 and 0.1 M $NaHCO_3$ aqueous solutions, in which most electrochemical measurements were done, were prepared using ultrapure Millipore water with a conductivity of 18.2 MΩ cm.

1.2 Apparatus and Methods

Field-emission scanning electron microscope (FE-SEM) (Hitachi S-4800, Japan) and (high resolution) transmission electron microscope (HRTEM) (JEM-2100, JEOL, Japan) were employed to characterize the morphology of the as-prepared photocathodes.

The optical absorption spectra of the Co_3O_4/CA were measured using a UV-diffusive reflective spectroscopy (Avalight DHS, Avantes, Netherlands) equipped with a deuterium/halogen lamp as the UV/visible light source.

The fluorescence spectra of $Ru(bpy)_2dppz$ were recorded on a Hitachi F-7000 photoluminescent spectrometer (Hitachi, Japan). For the fluorescence spectra, 5 mM $Ru(bpy)_2dppz$ in acetonitrile was used as the sample solution. The emission spectra were recorded with an excitation wavelength of 400 nm.

CHI660C electrochemical workstation (CH Instruments Inc., USA) with a conventional three-electrode system was applied to conduct all photoelectrochemical measurements. The light source was an LA-410UV lamp with UV cutoff (Hayashi, Japan) and a light intensity of 1 mW cm^{-2}. A PLS-SXE300 xenon lamp with UV cutoff (Perfect Light Co., Ltd., China) with a light density of 9 mW cm^{-2} was used in the photoelectrochemical CO_2 reduction.

Rotating disk electrode experiments were conducted on a CHI760C (CH Instruments Inc., USA) with a PINE rotator (Pine, USA). For these electrochemical experiments, an Ag/AgCl electrode with the saturated KCl solution acted as the reference electrode and a platinum foil as the counter electrode. The glassy carbon rotating electrode coated with $Ru(bpy)_2dppz$ or Co_3O_4 was the working electrode.

In comparison to those published, the potentials throughout the discussion in the textbody have been converted to ones with respect to the normal hydrogen reference electrode (NHE).

Both high performance liquid chromatogram (HPLC) equipped with UV detector (CP3900, Varian) and gas chromatogram (GC) equipped with a thermal conductive detector (GC7900,

Tech Comp, China) were adopted for quantitative determination of reduction products of CO_2 conversion on photocathodes.

1.3 Fabrication of Ru(bpy)$_2$dppz-Co$_3$O$_4$/CA photoelectrocatalytic interface

The preparation steps of such an interface, namely Ru(bpy)$_2$dppz-Co$_3$O$_4$/CA are demonstrated schematically in Scheme S1. Prior to the preparation of such an electrode, carbon aerogel (CA), Co$_3$O$_4$/CA, and Ru(bpy)$_2$dppz were synthesized.

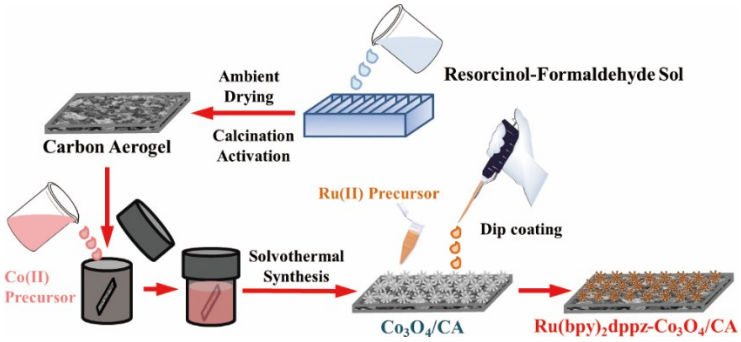

Scheme S1. Fabrication steps of Ru(bpy)$_2$dppz-Co$_3$O$_4$/CA concerted photoelectrocatalytic interface

Synthesis of CA Monolith bulky CA was prepared via ambient pressure resorcinol-formaldehyde (RF) drying method.[S1] In brief, resorcinol, formaldehyde, deionized water, and catalyst Na_2CO_3 were mixed with a molar ratio of 1:2:17.5:0.0008. Vigorous stirring led to the generation of a colorless and transparent solution. Subsequently, the solution was transferred to the glass molds with an interlayer distance of 5 mm. The gel was aged continuously at 30 °C for 1 day, 50 °C for 1 day, and 90 °C for 3 days. To exchange water content in the network of the gel, the as-formed organic RF gel was immersed in acetone for 3 days. The obtained orange gel was dried at ambient conditions and then pyrolyzed at 950 °C for 4 h under N_2 atmosphere. The gas flow rate was 200 mL min^{-1}. The black bulky monolith was then formed. To activate this monolith, the annealing was conducted at 850 °C for 4 h under the atmosphere of CO_2/N_2 (volume ratio = 4:1). The ramping rate was 5 °C min^{-1}. The as-formed black monolith was activated CA.

Synthesis of Ru(bpy)$_2$dppz A three-step approach was employed. Ru(bpy)$_2$Cl$_2$·H$_2$O and dipyrido[3,2-*a*:2′,3′-*c*]phenazine (dppz) were firstly synthesized. i) Synthesis of Ru(bpy)$_2$Cl$_2$·H$_2$O: In 50 mL DMSO, 7.8000 g RuCl$_3$·xH$_2$O, 9.3600 g pyridine and 8.4000 g LiCl were dissolved. The mixture was refluxed and stirred for 8 h. After cooling the mixture down to room temperature, 250 mL acetone was added. Keeping such a mixture at 0 °C for overnight led to the production of dark green crystals. They were obtained via filtering the mixture. After washing with 25 mL deionized water and ether for three times, the crystals were dried in vacuum. ii) Synthesis of dppz: In a 125 mL round-bottom flask, 4.0000 g 1,10-phenanthroline and KBr with equal masses were transferred. The mixture of concentrated sulfuric acid and nitric acid ($V_{\text{sulfuric acid}}$:$V_{\text{nitric acid}}$ = 40:20) was added dropwisely into the flask under magnetic stirring. The temperature after adding the acid mixture was kept at 80-85 °C for 3 h. After cooling down to room temperature, the mixture was transferred into 500 mL ice-water

mixture. The pH of the mixture was adjusted to 5-6 by adding 10 M NaOH. The products were extracted with 100 mL chloroform for three times, and then washed with deionized water. Na_2SO_4 anhydrate was utilized to absorb water during extraction for overnight. Removal of Na_2SO_4 was done by filtering and re-crystallizing the product with 50 - 100 mL ethanol. A yellow-orange and needle-like crystal was obtained. iii) Synthesis of $Ru(bpy)_2dppz$: In a 380 mL mixture of methanol-water ($V_{methanol}$:V_{water} = 1:2), 1.5400 g $Ru(bpy)_2Cl_2 \cdot H_2O$ and 0.9300 g dppz were dissolved. After refluxing such a solution for 4.5 h, its color was changed to heavy red. This heavy-red solution was concentrated to 10% by heating at 80 ^oC. Then 10 mL concentrated solution was diluted in 140 mL with deionized water. After boiling the solution for 10 min, raw products were cooled in iced water and further filtered. During filtering, 10% $NaBF_4$ solution was added. The products in filtrate were purified by recrystallization in methanol.

Fabrication of $Ru(bpy)_2dppz$-Co_3O_4/CA Chemical polymerization was utilized to decorate Co_3O_4/CA with $Ru(bpy)_2dppz$. In brief, 0.0040 g $Ru(bpy)_2dppz$ was dissolved in 1 mL acetonitrile solution, denoted as A. 0.0650 g $Fe(NO_3)_3 \cdot 9H_2O$ together with 8 μL pyrrole was dissolved in 1 mL ethanol. The mixture was denoted as B. Mixing A and B (with equal volumes) by shaking generated the stock solution for the electrode coating. One slide of Co_3O_4/CA was then coated with 200 μL stock solution dropwisely. Such a composite was dried at 60 °C for 5 min. After repeating such a coating procedure for 10 times, $Ru(bpy)_2dppz$-Co_3O_4/CA was fabricated.

Preparation of photocathode $Ru(bpy)_2dppz$-Co_3O_4/CA powders were connected on a copper plate (2×2 cm^2) with silver paste. Then a self-made alligator clip was soldered on to $Ru(bpy)_2dppz$-Co_3O_4/CA. The photocathode, namely $Ru(bpy)_2dppz$-Co_3O_4/CA coated electrocatalytic interface, was further sealed by water-proof silicone glue. The geometric area of working electrode was 1×1 cm^2.

Calculation and discussion of activation energy Due to a full coordination of the Ru(II) center inside of $Ru(bpy)_2dppz$ molecular catalyst, further binding of CO_2 to the Ru(II) center is not possible. The electron transfer from $Ru(bpy)_2dppz$ to CO_2 thus obeys the outer-sphere electron transfer mechanism. In other words, CO_2 will be firstly activated and then proton coupled electron transfer occurs, of which pattern belongs to the dissociative electron transfer mode. Then, the activation energy, ΔG^*, can be calculated using the equation of:

$$\Delta G^* = \Delta G_0^* \left(1 + \frac{\Delta G^o}{4\Delta G_0^*}\right)^2 \quad (1)$$

where ΔG_o^* is the intrinsic barrier and ΔG^o is the apparent free energy change for the electrochemical reaction. ΔG^o can be calculated through classical thermodynamics:

$$\Delta G^o = nF(E - E^o) \quad (2)$$

Assuming one electron transfer mechanism during CO_2 reduction, the value of ΔG_o^* can be calculated through the following equation:

$$\alpha = 0.5 + \frac{F}{8\Delta G_0^*}\left(E - E^\circ\right) \quad (3)$$

where α is the charge transfer coefficient, F (=96500 C mol^{-1}) the faraday constant, E is the applied potential, and E^o is the standard redox potential for CO_2 to formate. In our case, E^o was -0.61 V vs. NHE. According to the Tafel equation, the charge transfer coefficient, α, can be calculated by the following equation:

$$b = \frac{2.303RT}{\alpha F} \quad (4)$$

where b is the Tafel slope, R (= 8.3145 J mol^{-1} K^{-1}) is the gas constant, and T is the Kelvin temperature. According to the results shown in Fig. 3c, b was calculated to be 145 mV dec^{-1} for $Ru(bpy)_2dppz$-Co_3O_4/CA.

Using equation (4) α was calculated to be 0.408. Using equation (2) and (3) and a value of E = 0.59 V (vs. NHE), obtained from the red plot in Fig. 1a, ΔG_o^* is to be 2.622 kJ mol^{-1}, leading to a ΔG^* value of 1.047 kJ mol^{-1}.

2. Supplementary Results

Table S1. CO_2 adsorption capacity and electrochemically active surface area of Co_3O_4/FTO, Co_3O_4/CA and Ru(bpy)$_2$dppz-Co_3O_4/CA photocathodes.

	Co_3O_4/FTO	Co_3O_4/CA	Ru(bpy)$_2$dppz-Co_3O_4/CA
m [mg cm^{-2}]	5	8	4
S [cm^2]	6.14×10^{-3}	1.64×10^{-2}	1.64×10^{-2}
S_{EASA} [cm^2]	316	8015	2030
Γ_{ads} [cm^2]	3.88×10^{-3}	1.99	7.69
Γ_{ads}/A [nmol cm^{-2}]	7.76×10^{-2}	39.8	154
Γ_{ads}/S_{EASA} [pmol cm^{-2}]	1.23×10^{-2}	0.248	3.79
Γ_{ads}/m [μmol g^{-1}]	1.55×10^{-2}	4.97	38.5

m: loading amount catalyst;
S: active surface area determined by cyclic voltammogram in 5 mM $Fe(CN)_6^{3-/4-}$;
S_{EASA}: electrochemical active surface area;
Γ_{ads}: amount of CO_2 adsorbed on photocathode;
A, geometric electrode area (= 0.05 cm^2)

Table S2. Comparison of peak current densities (normalized by geometric area or loading amount of the catalyst) and corresponding onset potentials on Co_3O_4/FTO, Co_3O_4/CA and Ru(bpy)$_2$dppz-Co_3O_4/CA photocathodes.

		[a]Co_3O_4/FTO	[b]Co_3O_4/CA	[c]Ru(bpy)$_2$dppz-Co_3O_4/CA
$j_{A,\mathrm{peak}}$ [mA cm^{-2}] @ E_{onset} [V] (peak current density normalized by geometric area)				
N_2,	EC	0.095 @ -0.77	1.110 @ -0.59	3.450 @ -0.56
N_2,	PEC	0.206 @ -0.70	1.470 @ -0.57	4.600 @ -0.50
CO_2,	EC	0.061 @ -0.70	1.730 @ -0.59	5.230 @ -0.50
		0.271 @ -0.81	0.789 @ -0.72	
CO_2,	PEC	0.103 @ -0.67	1.690 @ -0.53	8.040 @ -0.45
		0.534 @ -0.74	0.868 @ -0.65	
$j_{m,\mathrm{peak}}$ [mA mg^{-1}] @ E_{onset} [V] (peak current density normalized by the loading amount of catalyst)				
N_2,	EC	0.019 @ -0.77	0.139 @ -0.59	0.863 @ -0.56
N_2,	PEC	0.041 @ -0.70	0.184 @ -0.57	1.150 @ -0.50
CO_2,	EC	0.012 @ -0.70	0.216 @ -0.59	1.308 @ -0.50
		0.054 @ -0.81	0.099 @ -0.72	
CO_2,	PEC	0.021 @ -0.67	0.211 @ -0.53	2.010 @ -0.45
		0.107 @ -0.74	0.109 @ -0.65	

EC: electrochemical condition;
PEC: photoelectrochemical condiction.
$j_{A,\mathrm{peak}}$: peak current density normalized by the geometric area of the photocathode
$j_{m,\mathrm{peak}}$: peak current density normalized by the loading amount of the catalyst;
E_{onset}: onset potential
A: geometric electrode area (= 0.05 cm^2)

Table S3. Turnover number (TON) of photoelectrochemical CO_2 reduction into formate on Co_3O_4/FTO, Co_3O_4/CA, Ru(bpy)$_2$dppz/CA and Ru(bpy)$_2$dppz-Co_3O_4 photocathodes under various potentials for 8 h.

E vs. NHE / V	$TON_{formate}$			
	Co_3O_4/FTO	Co_3O_4/CA	Ru(bpy)$_2$dppz/CA	Ru(bpy)$_2$dppz-Co_3O_4/CA
0	2.6	2.0	5.3	121.1
-0.2	3.5	4.5	5.7	205.3
-0.4	4.9	8.6	18.9	681.1
-0.5	5.8	17.6	38.7	908.6
-0.6	5.8	22.3	39.7	978.7
-0.7	9.3	24.0	48.3	1179.1
-0.8	10.1	26.6	57.5	1334.4
-0.9	10.7	30.2	77.8	1771.2
-1.0	11.2	35.6	89.3	1964.9

Table S4. Turnover frequency (TOF) photoelectrochemical CO_2 reduction into formate on Co_3O_4/FTO, Co_3O_4/CA, Ru(bpy)$_2$dppz/CA and Ru(bpy)$_2$dppz-Co_3O_4 photocathodes under various potentials for 8 h.

E vs. NHE / V	$TOF_{formate}$ [h^{-1}]			
	Co_3O_4/FTO	Co_3O_4/CA	Ru(bpy)$_2$dppz/CA	Ru(bpy)$_2$dppz-Co_3O_4/CA
0	0.32	0.27	0.67	15
-0.2	0.43	0.55	0.71	25
-0.4	0.61	1.1	2.4	85
-0.5	0.73	2.2	4.8	113
-0.6	0.85	2.8	5.0	122
-0.7	1.2	3.0	6.0	147
-0.8	1.3	3.3	7.2	166
-0.9	1.3	3.8	9.7	221
-1.0	1.4	4.4	11.2	245

The equation for the calculation of TON and TOF:

$$\mathrm{TON} = \frac{\text{mols of formate produced}}{\text{mols of catalysts used}} \tag{5}$$

$$\mathrm{TOF} = \frac{\mathrm{TON}}{\text{reaction time}} \tag{6}$$

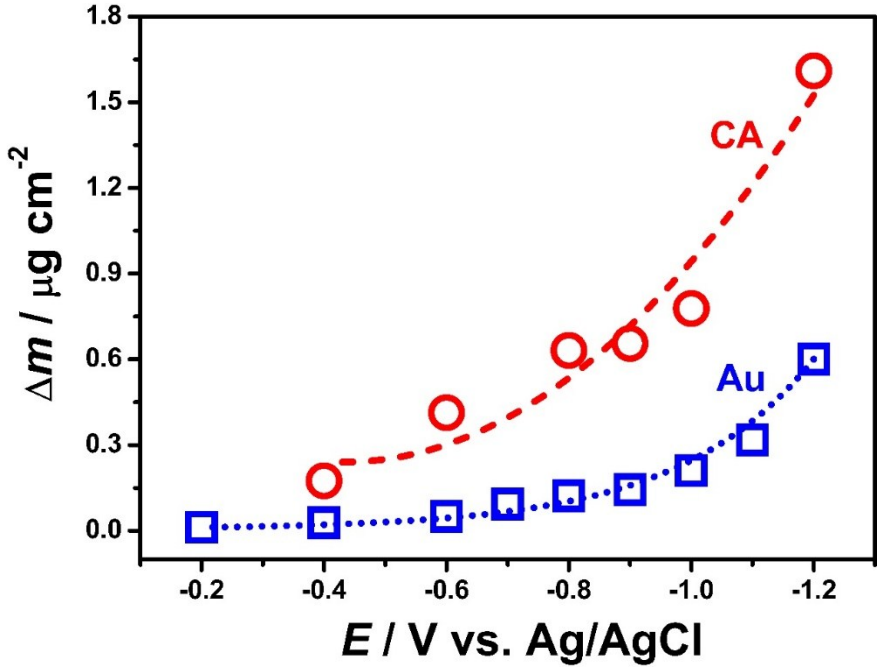

Fig. S1. Variation of Δm as a function of applied potentials on the Au crystal before (squares) and after (circles) being coated with CA.

In EQCM experiments, Δm, was calculated according to Sauerbrey's equation:[S2]

$$\Delta m = -S \cdot \Delta f \tag{7}$$

where Δm is the mass addition of the electrode (namely the mass difference before and after CO_2 adsorption), S (= 5.29 ng cm^{-2} Hz^{-1}) is the calibrated sensitivity factor and Δf is the change of the frequencies during measurements.

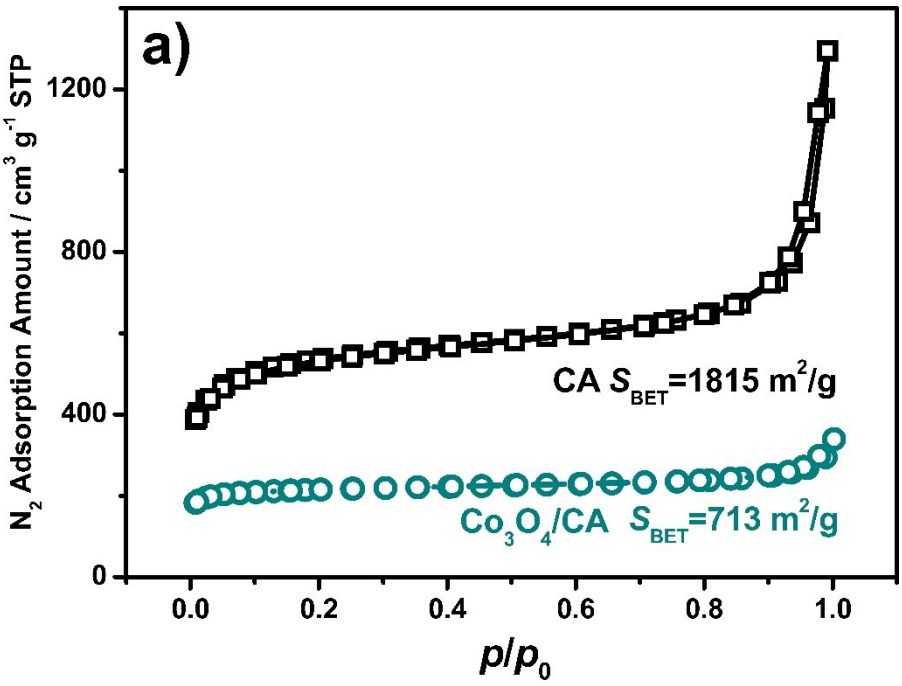

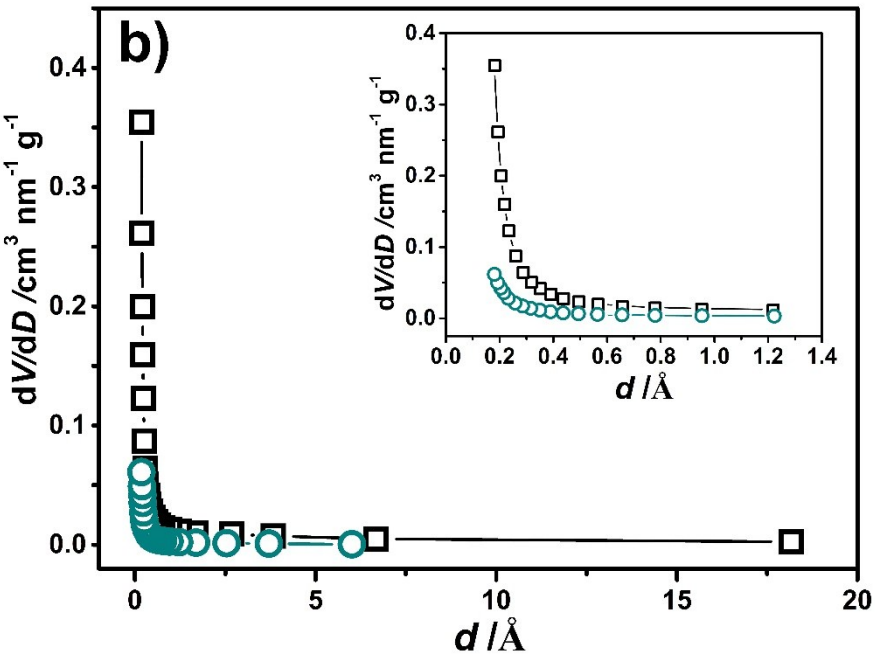

Fig. S2. (a) N_2 adsorption/desorption isotherm and (b) Barrett-Joyner-Halenda (BJH) pore size distribution of Co_3O_4/CA (circles) and CA (squares). Inset of (b): Magnification in the 0.15-1.2 Å region.

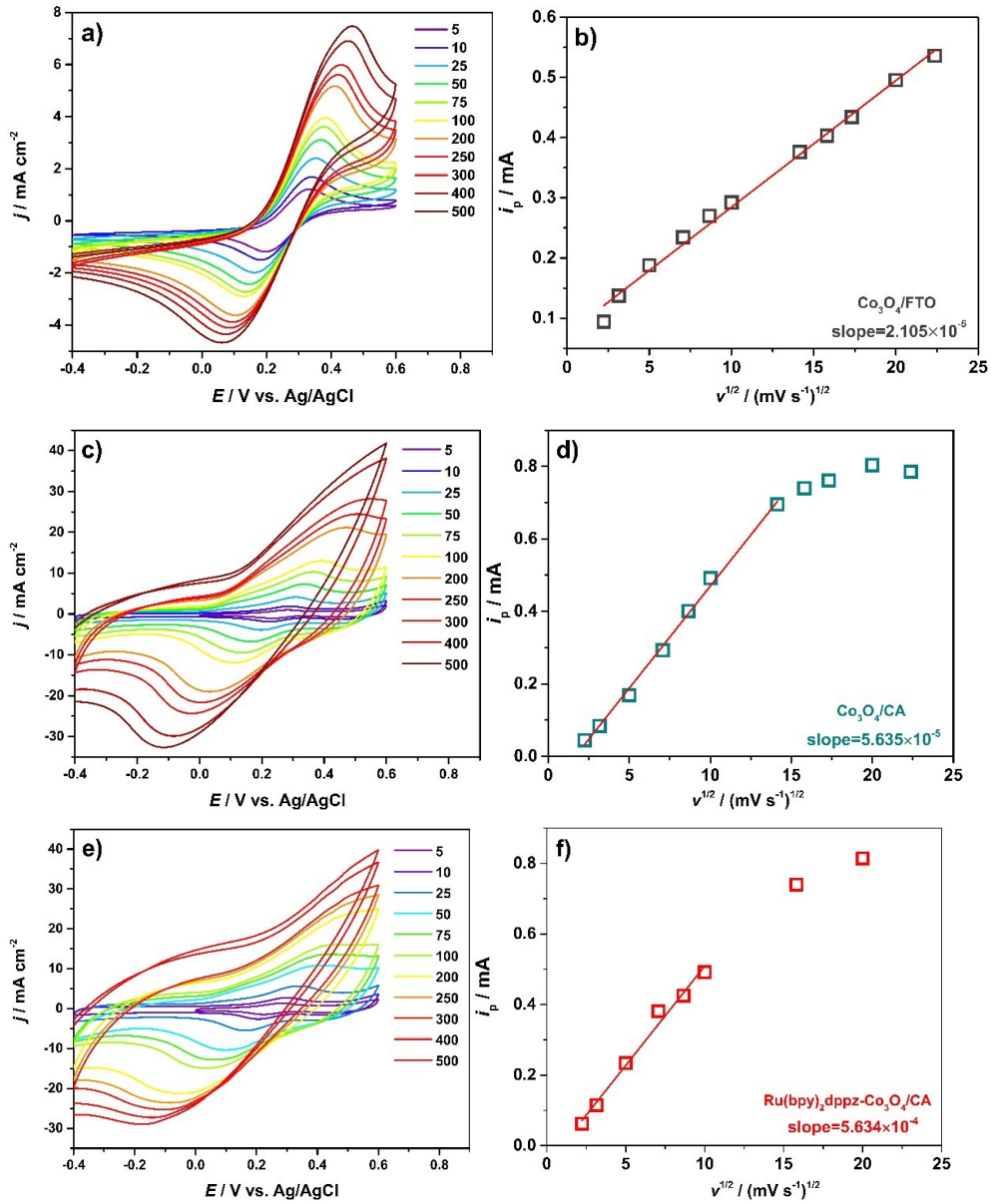

Fig. S3 Cyclic voltammograms of 5 mM $Fe(CN)_6^{3-/4-}$ in 0.1 M KCl on (a) Co_3O_4/FTO, (c) Co_3O_4/CA and (e) $Ru(bpy)_2$dppz-Co_3O_4/CA photocathodes at the scan rate of 5, 10 25, 50, 75, 100, 200, 250, 300, 400, and 500 mV s^{-1}. Variation of peak current densities as a function of the square root of scan rates for (b) Co_3O_4/FTO, (d) Co_3O_4/CA, and (f) $Ru(bpy)_2$dppz-Co_3O_4/CA.

The real active area can be calculated through Randles-Sevcik equation:

$$i_p = 2.69\times10^5 n^{3/2} A D^{1/2} C v^{1/2} \quad (8)$$

where i_p is the peak current, n is the electron transferred (n=1 in current case), A is the active electrode area, D is the diffusion constant of ferrous cynide (D=6.7×10^{-6} cm^2 s^{-1}), C is the concentration of ferrous cyanide, and v is the scan rate. Linear fittings gave the slopes of 2.105×10^{-5}, 5.635×10^{-5}, and 5.634×10^{-5} in Fig. 3(b), (d) and (f), which are for Co_3O_4/FTO, Co_3O_4/CA and $Ru(bpy)_2$dppz-Co_3O_4/CA, respectively. Therefore, the active electrode area is 6.14×10^{-3}, 1.64×10^{-2}, and 1.64×10^{-2} cm^2 for Co_3O_4/FTO, Co_3O_4/CA and $Ru(bpy)_2$dppz-Co_3O_4/CA, respectively. These values are also tabulated in Table S1.

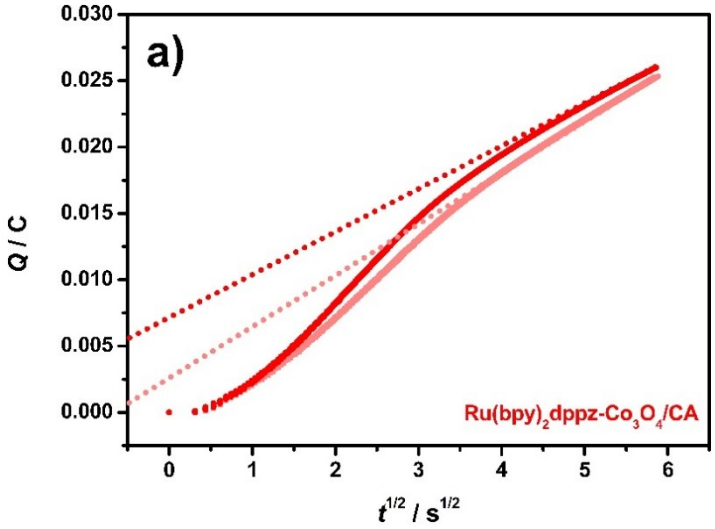

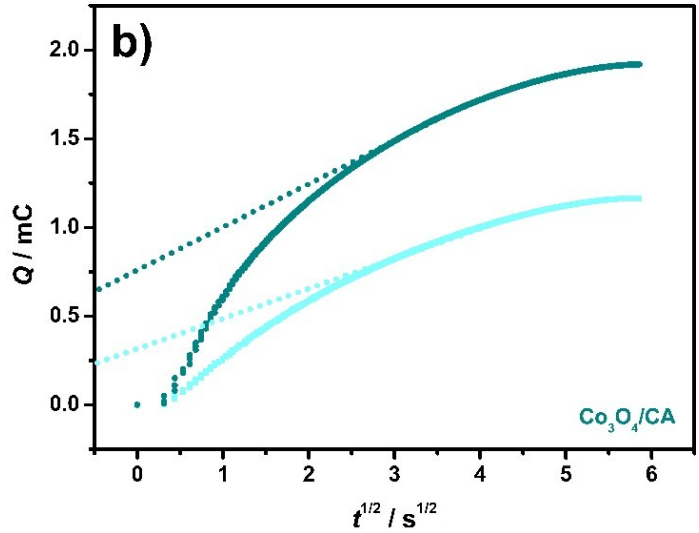

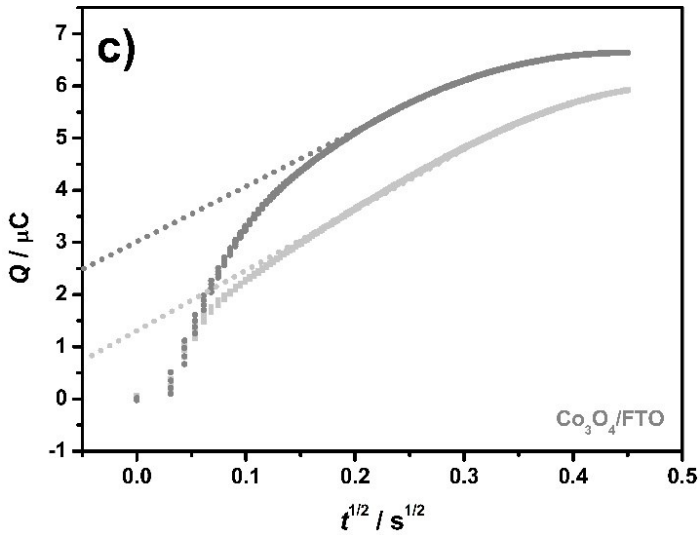

Fig. S4. Chronocoulometry of (a) $Ru(bpy)_2dppz$-Co_3O_4/CA, (b) Co_3O_4/CA, and (c) Co_3O_4/FTO in N_2 (light-colored line) / CO_2 (dark-colored line) purged 0.1 M Na_2SO_4. The potential was stepped from 0 to -1.0 V vs. Ag/AgCl. The pulse width was 100 s for both $Ru(bpy)_2dppz$-Co_3O_4/CA and Co_3O_4/CA, and 1 s for Co_3O_4/FTO.

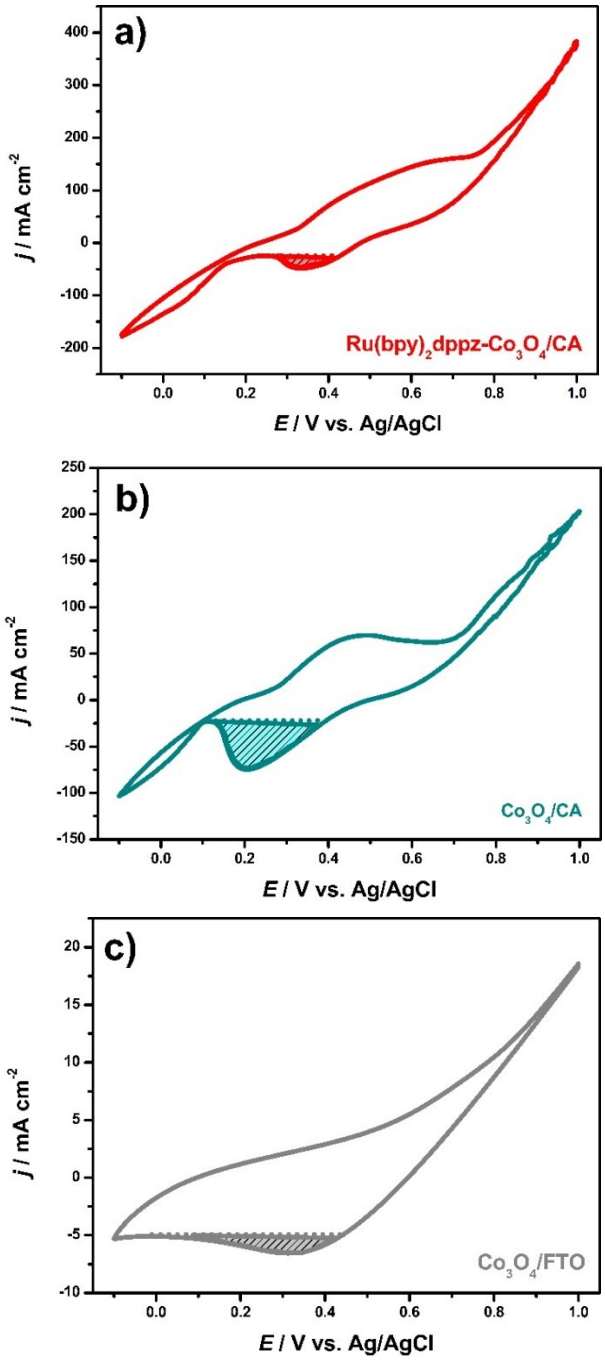

Fig. S5. Cyclic voltammograms of (a) $Ru(bpy)_2$ dppz-Co_3O_4/CA, (b) Co_3O_4/CA, and (c) Co_3O_4/FTO in 1 M NaOH at a scan rate of 50 mV s^{-1}.[S3]

The electrochemically active surface area (S_{EASA}) of the electrode was calculated using the equation of[S3]

$$S_{EASA} = \frac{A}{v \cdot C_{ref}} \tag{9}$$

where A is the integrated area of the reduction peak in the cyclic voltammogram (the shade area shown in Fig. S5), v is the scan rate, and C_{ref} (=60 μF cm^{-2}) is the reference capacity of Co_3O_4.[S3]

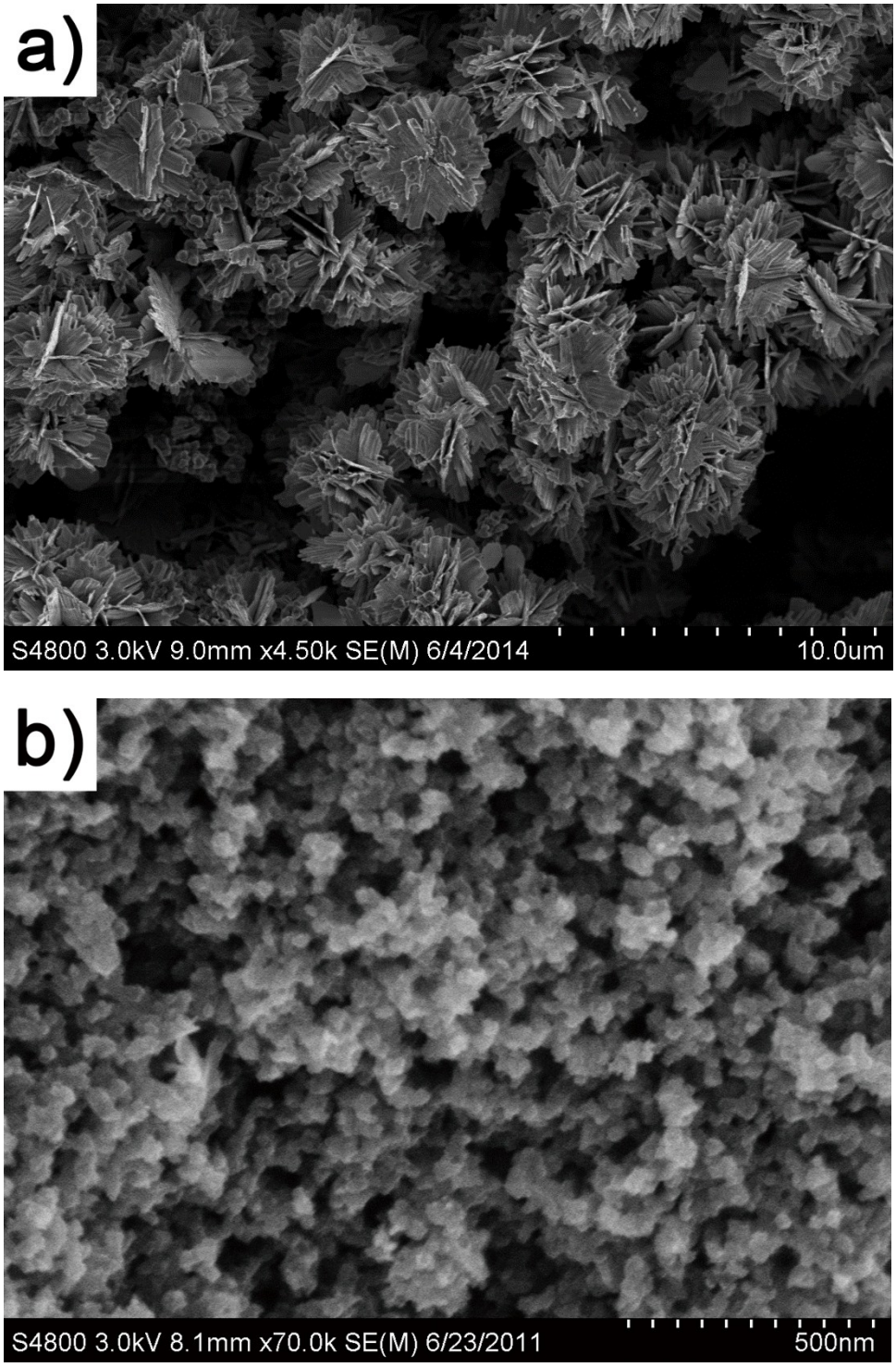

Fig. S6. SEM images of (a) Co_3O_4/CA and (b) magnified Co_3O_4 micro-flowers.

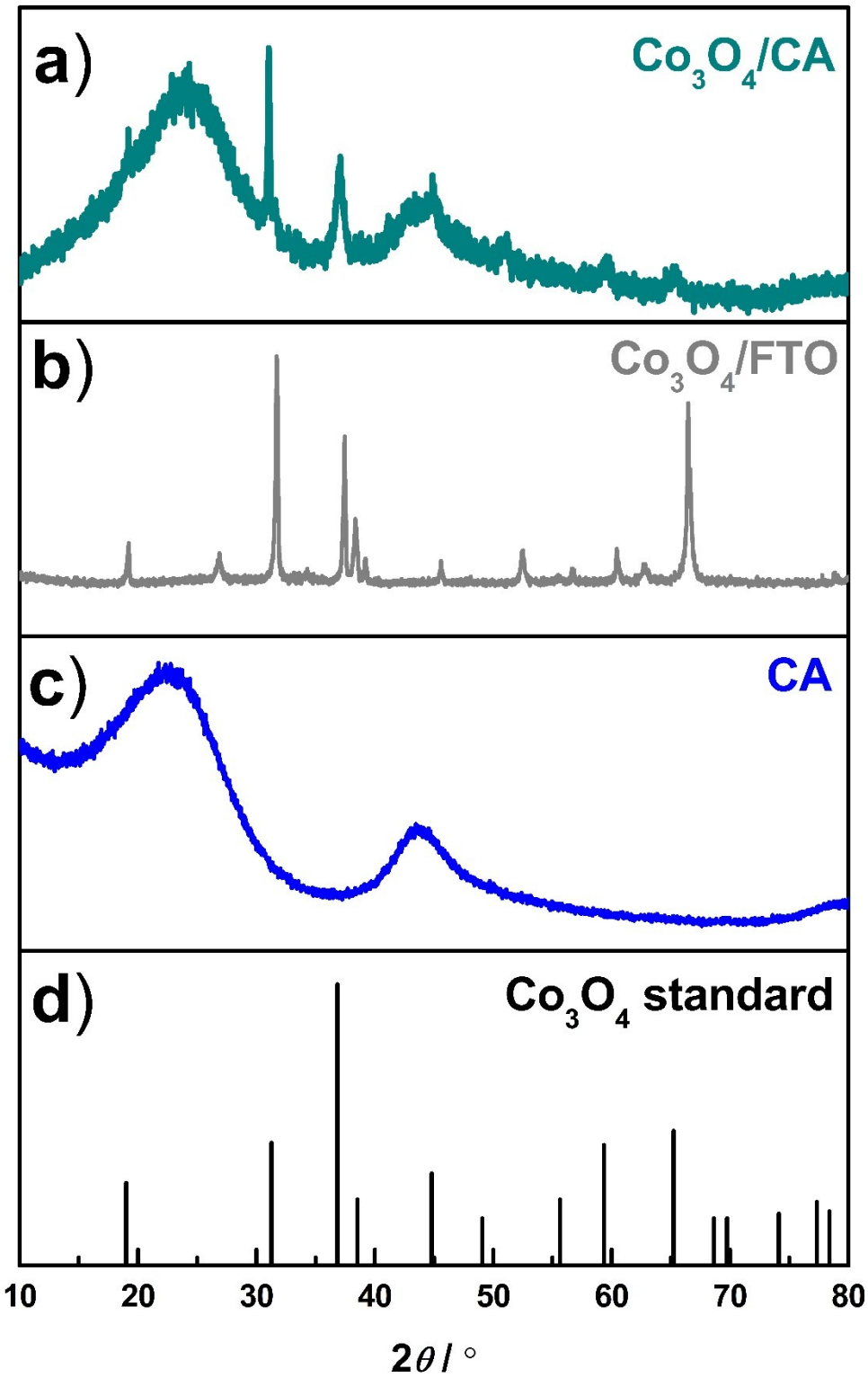

Fig. S7. XRD patterns of (a) Co_3O_4/CA, (b) Co_3O_4/FTO, (c) CA, and (d) standard XRD patterns of Co_3O_4.

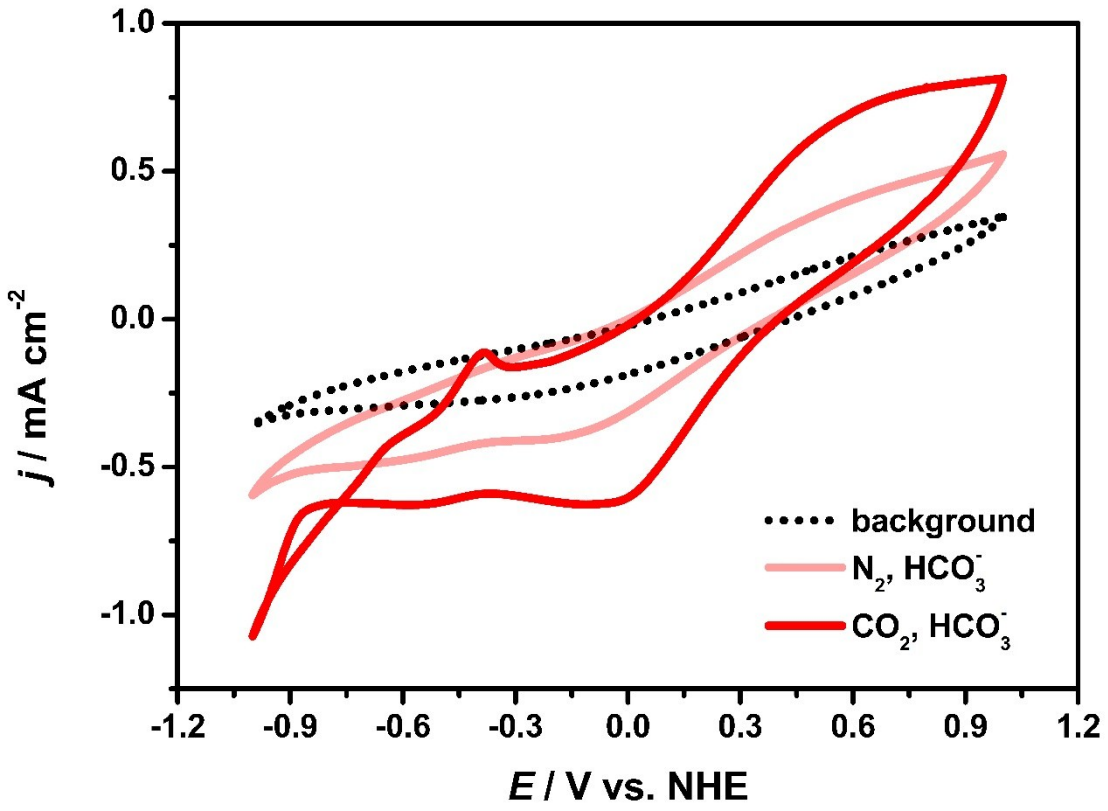

Fig. S8. Cyclic voltamograms of $Ru(bpy)_2dppz$/FTO at a scan rate of 50 mV s^{-1} in N_2 purged Na_2SO_4 (black-dotted line) and $NaHCO_3$ (pink-solid line) as well as in CO_2 saturated $NaHCO_3$ (red-solid line). The concentration of the solutions was 0.1 M.

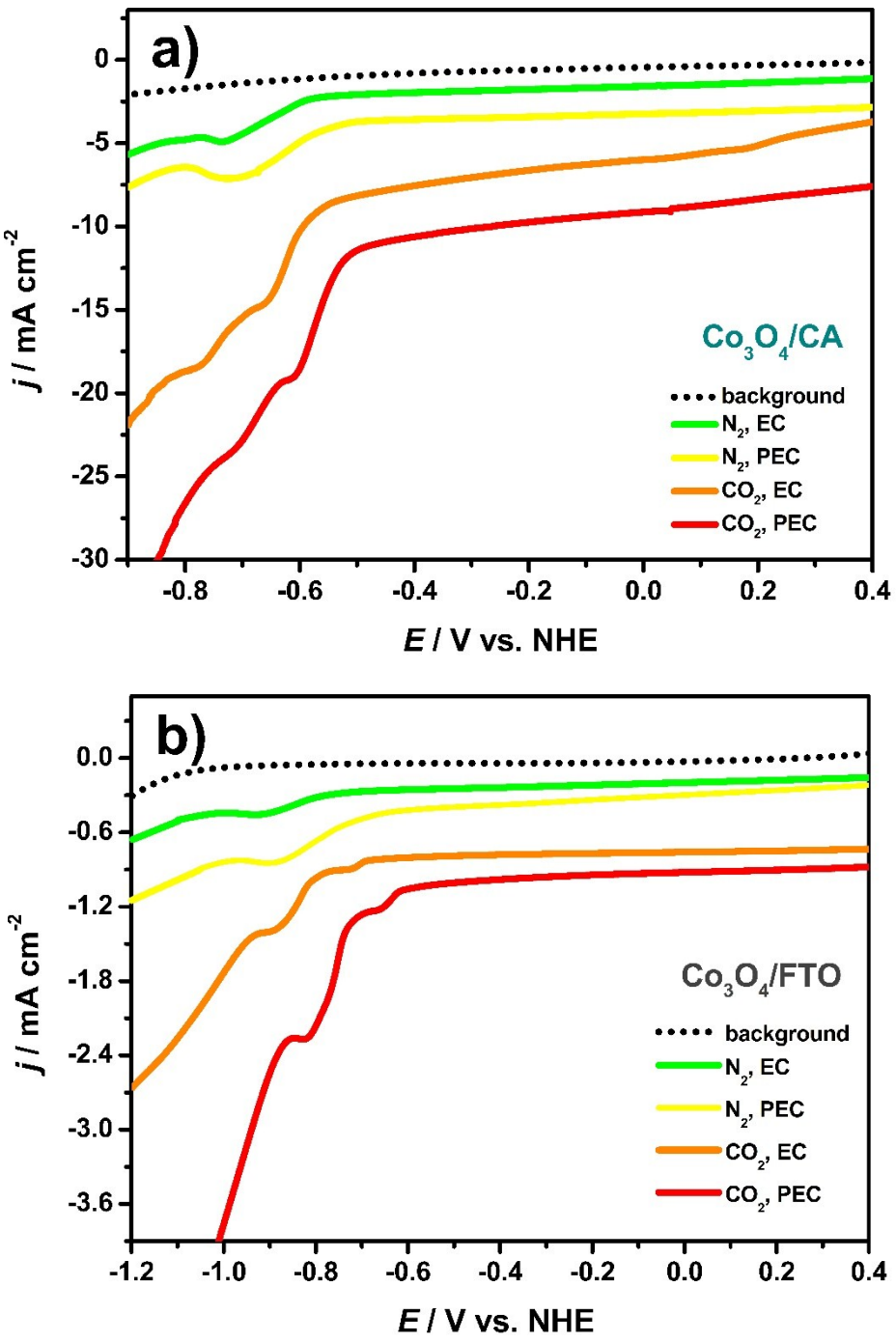

Fig. S9. Linear sweep voltamograms on (a) Co_3O_4/CA and (b) Co_3O_4/FTO at a scan rate of 50 mV s^{-1} in N_2 purged 0.1 M Na_2SO_4 (black dotted line), N_2 purged 0.1 M $NaHCO_3$ without (green) / with (yellow) irradiation, CO_2 saturated 0.1 M $NaHCO_3$ without (orange) / with (red) irradiation.

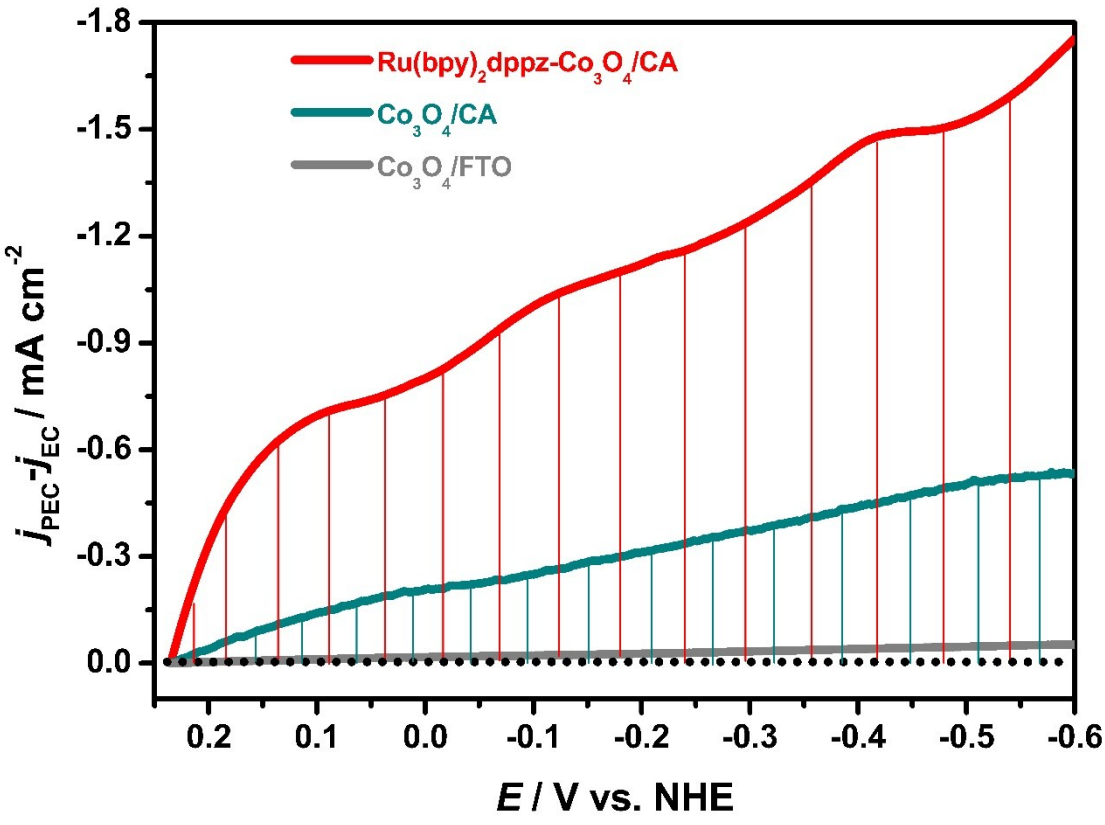

Fig. S10. The variation of j_{PEC}-j_{EC} on Ru(bpy)$_2$dppz-Co_3O_4/CA (red), Co_3O_4/CA (cyan) and Co_3O_4/FTO (gray) as a function of the potentials applied. The values of j_{PEC}-j_{EC} were calculated from linear sweep voltammograms conducted in 0.1 M Na_2SO_4 at a scan rate of 50 mV s^{-1}.

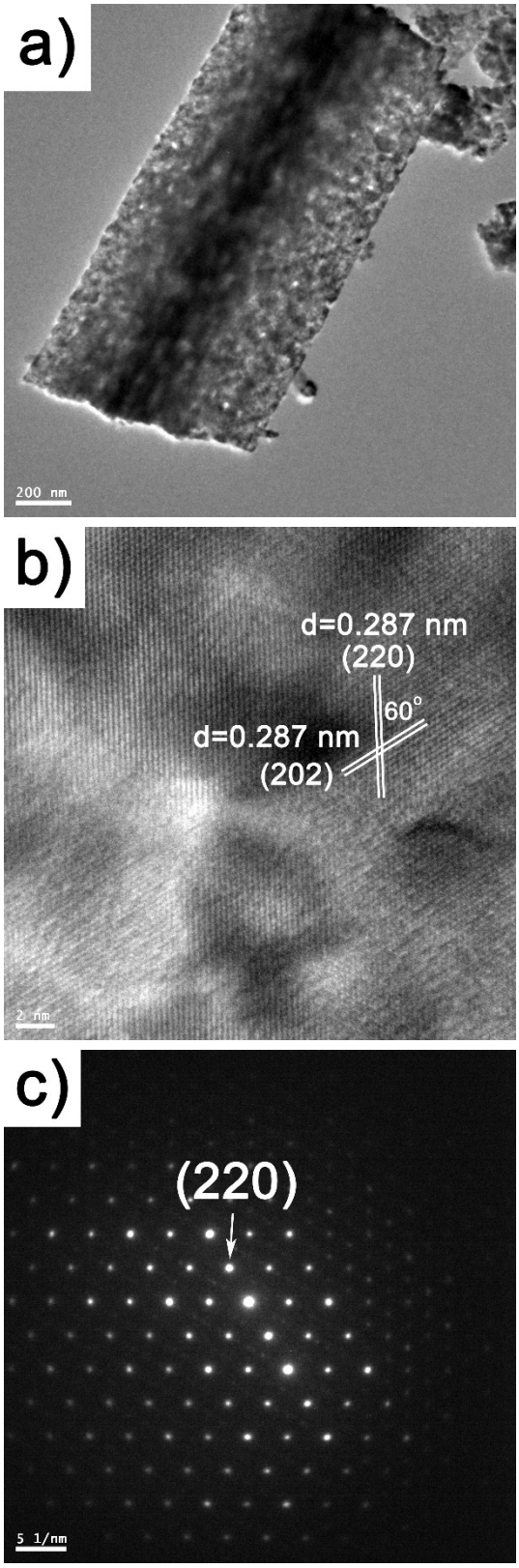

Fig. S11. (a) TEM image of a single petal on Co_3O_4 micro-flowers; (b) HRTEM pattern of petal region of a Co_3O_4 micro-flower; and (c) selected area electron diffraction pattern of petal region.

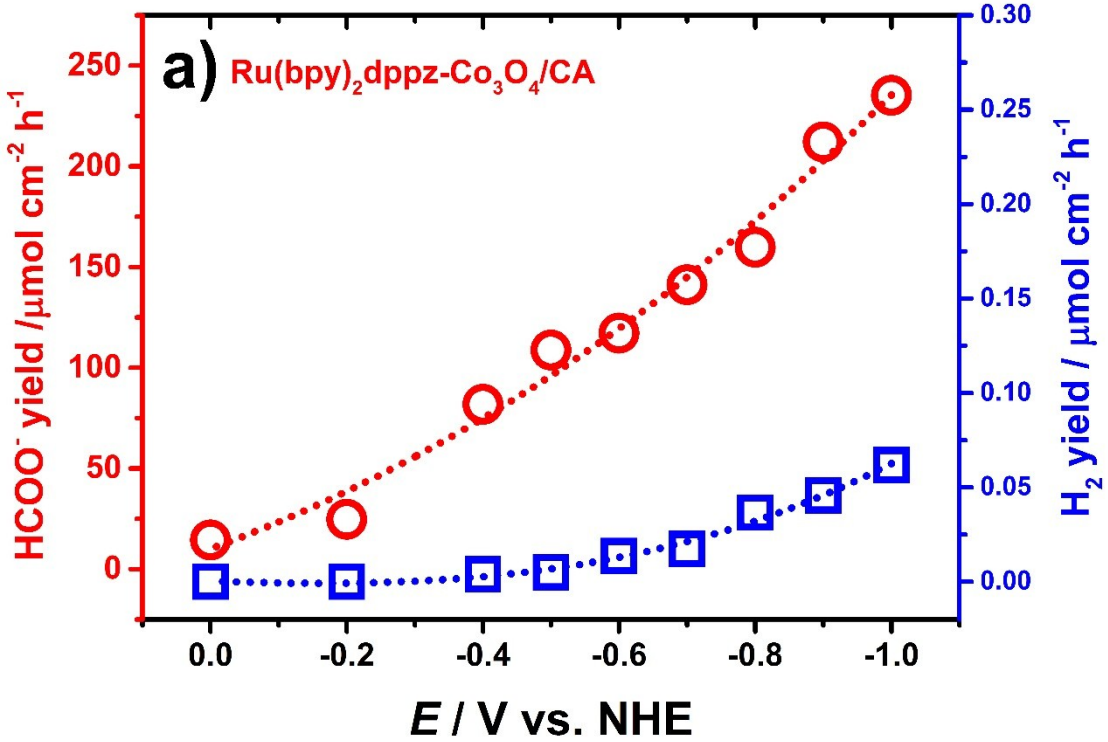
a) Ru(bpy)2dppz-Co3O4/CA
HCOO- yield /μmol cm-2 h-1
H2 yield / μmol cm-2 h-1
E / V vs. NHE
250
200
150
100
50
0
0.30
0.25
0.20
0.15
0.10
0.05
0.00
0.0
-0.2
-0.4
-0.6
-0.8
-1.0

1

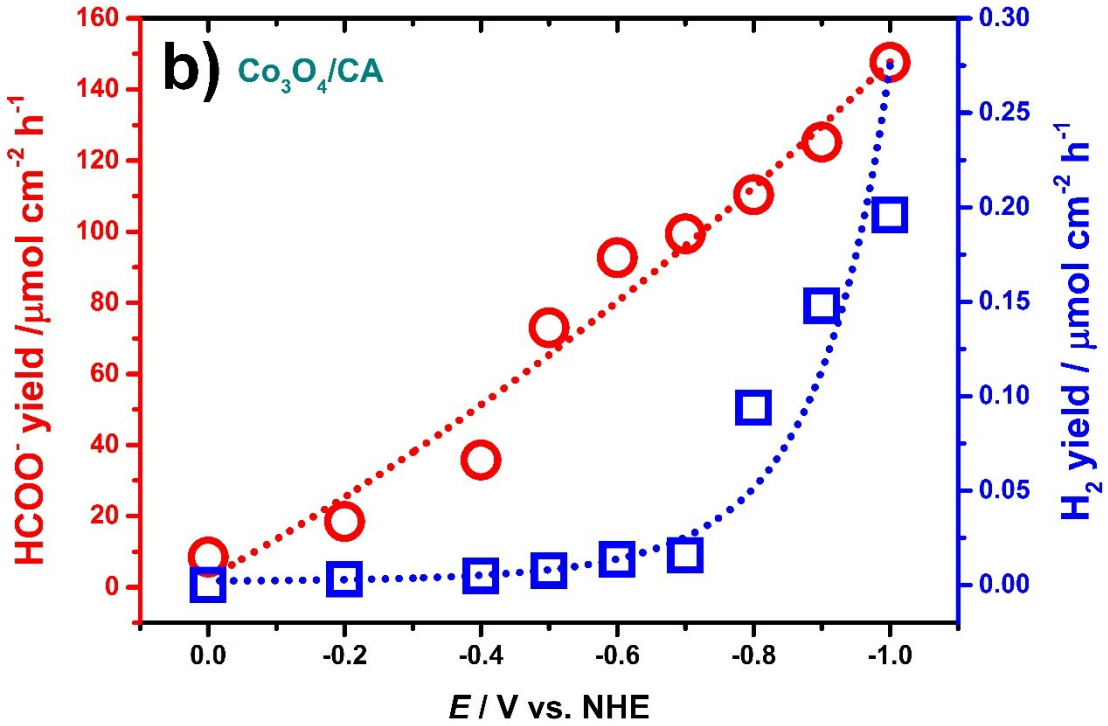
b) Co3O4/CA
HCOO- yield /μmol cm-2 h-1
H2 yield / μmol cm-2 h-1
E / V vs. NHE
160
140
120
100
80
60
40
20
0
0.30
0.25
0.20
0.15
0.10
0.05
0.00
0.0
-0.2
-0.4
-0.6
-0.8
-1.0

2

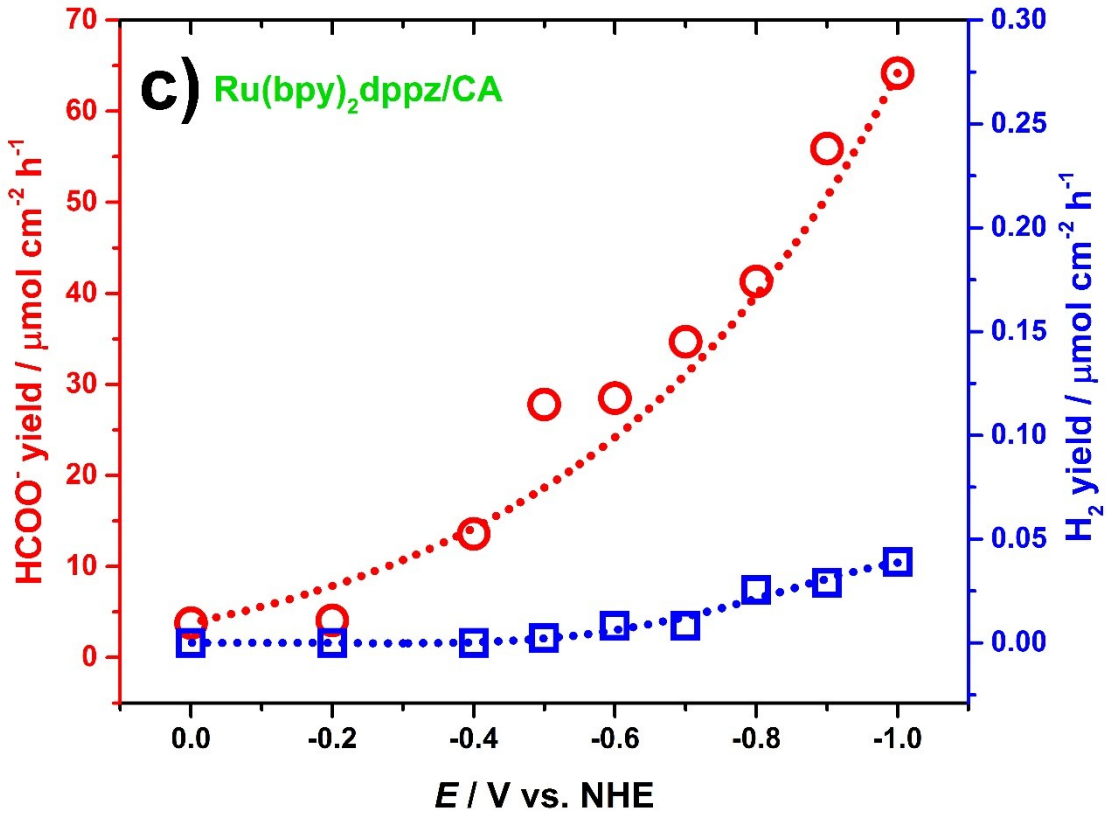

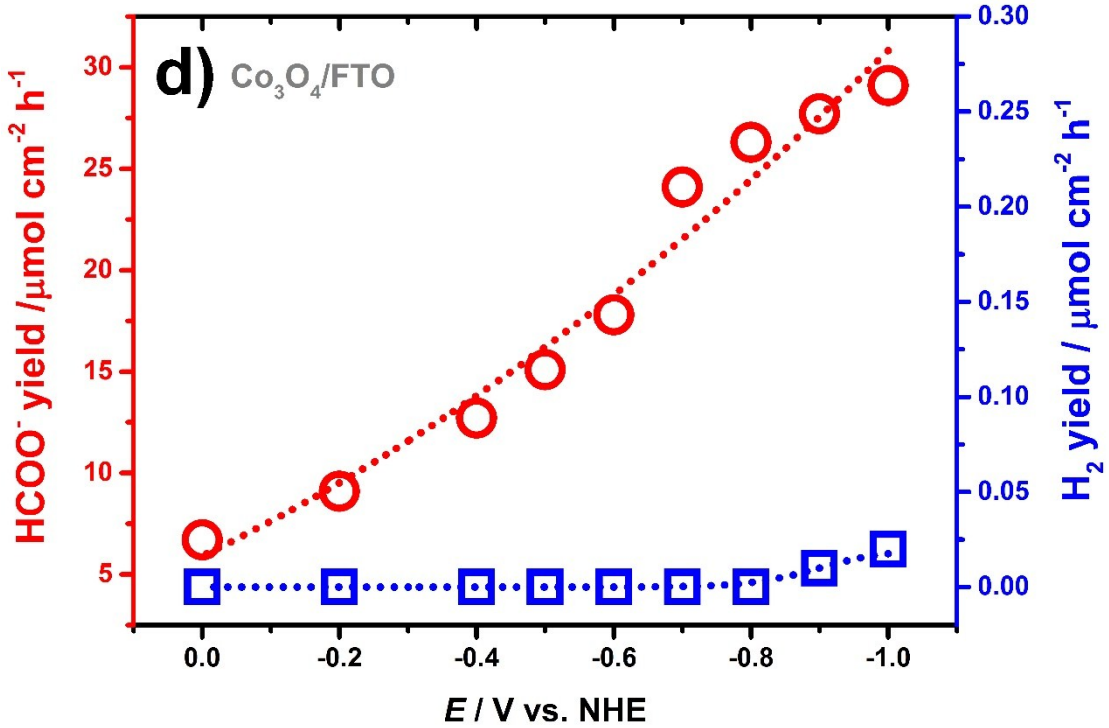

Fig. S12. Variation of yield rates of formate (red circle) and hydrogen (blue square) on the $Ru(bpy)_2dppz$-Co_3O_4/CA(a), Co_3O_4/CA (b), $Ru(bpy)_2dppz$/CA (c) and Co_3O_4/FTO (d) as a function of the applied potentials.

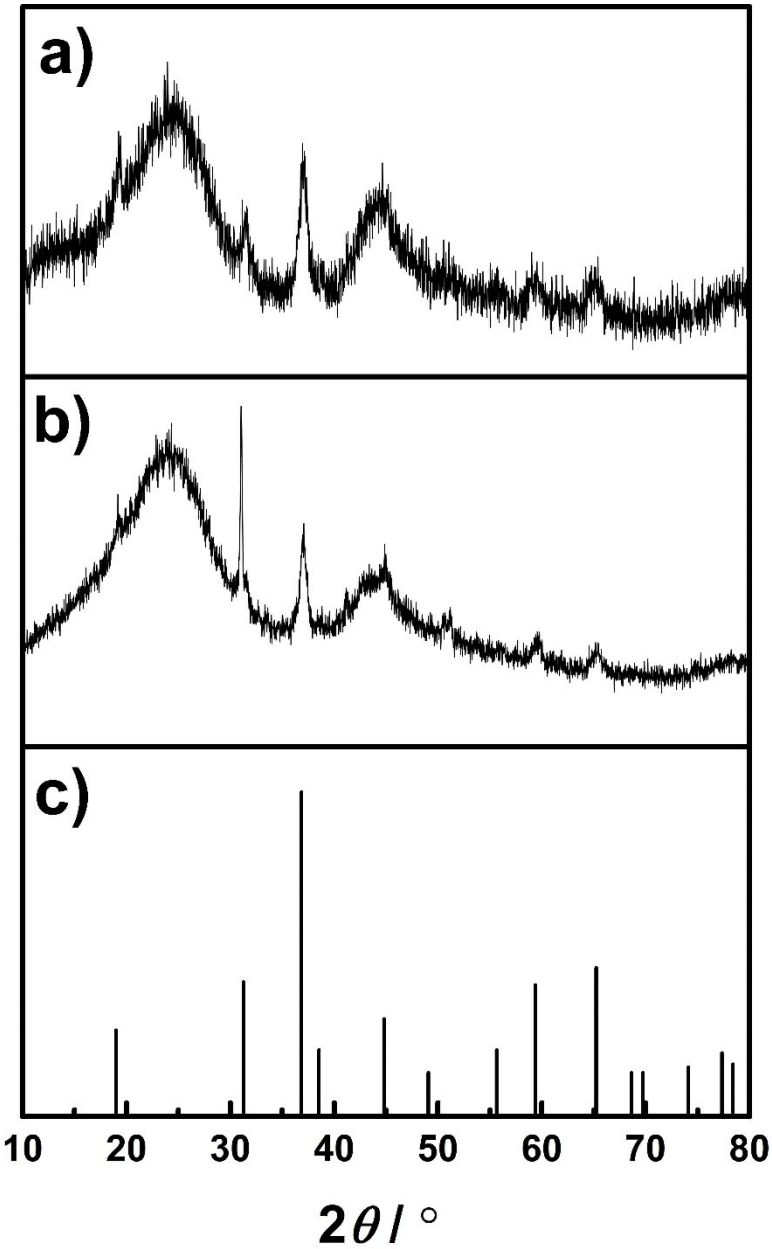

Fig. S13. XRD patterns of $Ru(bpy)_2dppz$-Co_3O_4/CA before (a) and after (b) photoelectrochemical CO_2 reduction for 8 h. c) Standard XRD patterns of Co_3O_4.

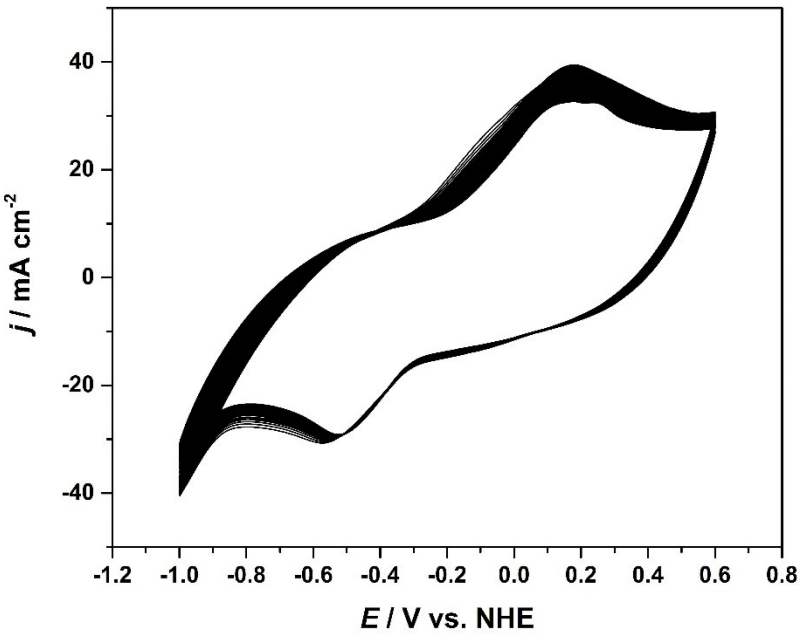

Fig S14. 100 continuous cyclic voltammograms of $Ru(bpy)_2dppz$-Co_3O_4/CA obtained at a scan rate of 50 mV s^{-1} in CO_2 saturated $NaHCO_3$ (0.1 M).

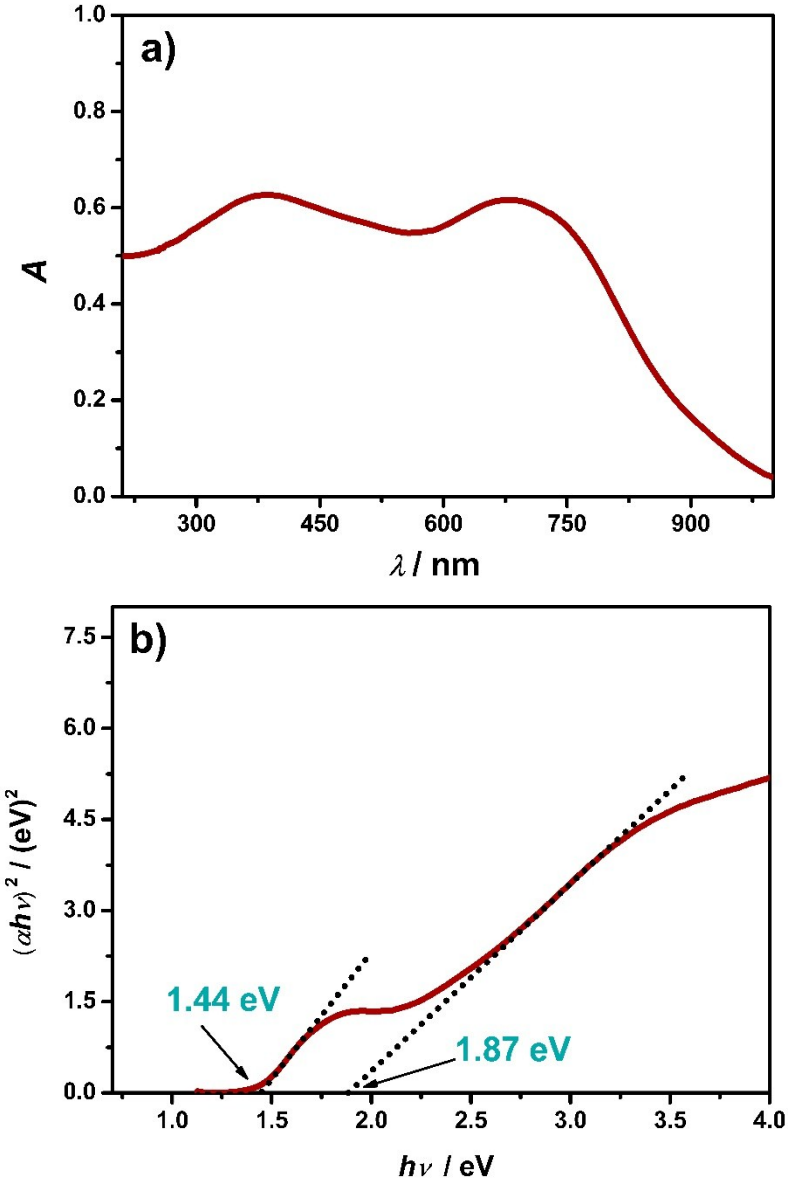

Fig. S15. UV-diffusive reflective spectrum (a) and the corresponding Tauc plot (b) of Co_3O_4/CA.

Tauc plot was converted according to the Tauc equation:[S4]

$$\alpha h\nu = A(h\nu - E_g)^{\frac{1}{n}} \tag{10}$$

where α is the absorption coefficient of Co_3O_4, h is the Planck's constant, ν is the frequency of incident light, and E_g is the band gap of Co_3O_4. Since the transition belongs to direct transition for Co_3O_4, then n is equal to 2.

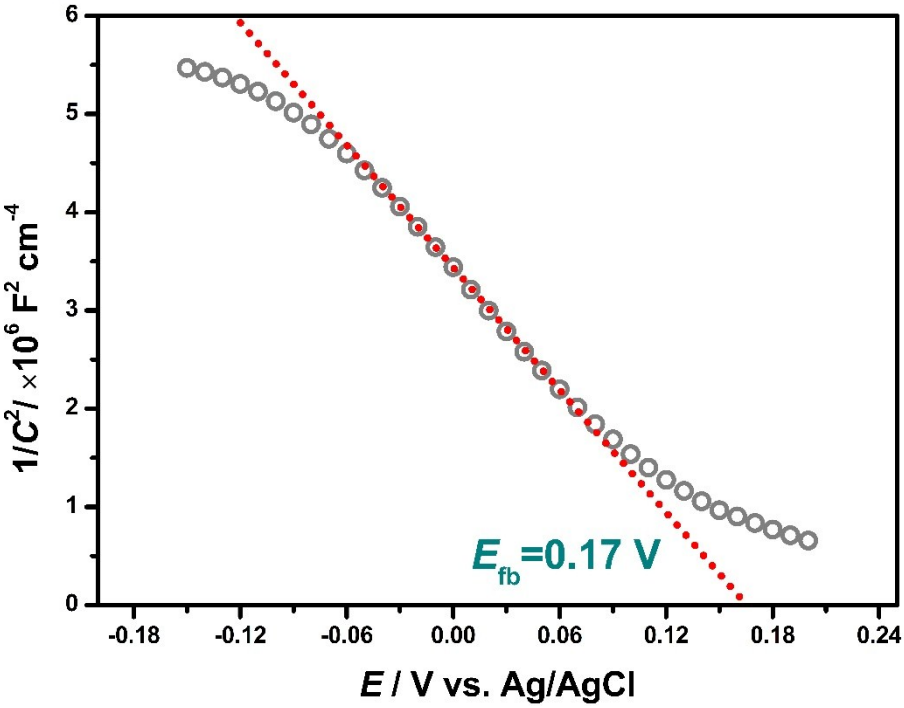

Fig. S16. Mott-Schottky plot of Co_3O_4/CA in 0.1 M Na_2SO_4 at a frequency of 1.0 kHz.

Mott-Schottky equation was employed to calculate the built-in potential of the flat-band potential of Co_3O_4 in the form of[S5]

$$\frac{1}{C^2} = \frac{2}{\varepsilon_0 \varepsilon_r A^2 N_B}(V - V_{FB} - \frac{kT}{e}) \quad (11)$$

where C is the space charge capacity (F), $\mathcal{E}_o$ (= 8.854×10^{-12} F m^{-1}) is the dielectric constant of vacuum, V is the applied potential (V), V_{FB} is the flat band potential (V), A is the electrode area (cm^2), N_B is the carrier concentration of Co_3O_4, k (=8.6173324×10^{-5} eV K^{-1}) is the Boltzmann's constant, T is the absolute temperature, and q is (=1.60×10^{-19} C) the elemental charge. $\mathcal{E}_r$ is 12.9 for Co_3O_4.[S6]

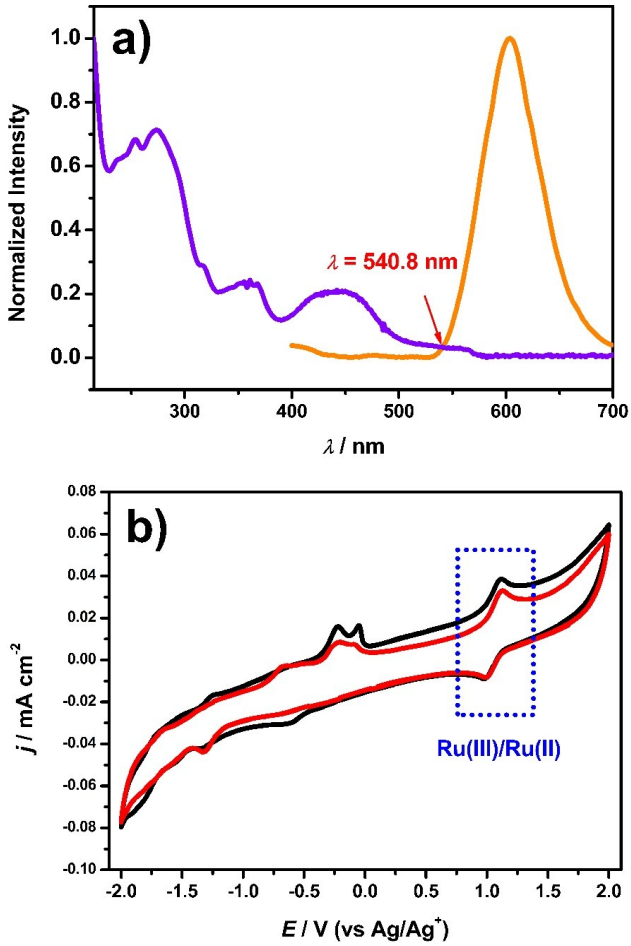

Fig. S17. (a) Imposing of UV-Vis absorption spectrum (purple) and corresponding fluorescent spectrum of 5 mM $Ru(bpy)_2dppz$ in MeCN; (b) Cyclic voltamograms of 5 mM $Ru(bpy)_2dppz$ at a scan rate of 100 mV s^{-1} in MeCN containing 0.1 M $TBAPF_6$ in the absence and presence of CO_2.

Here, MeCN was chosen as the solvent for electrochemical characterization of $Ru(bpy)_2dppz$. The Ru molecular catalyst we used was not water-soluble and hence its electrochemical properties, or related energies, can be only obtained from the results obtained in organic solvents[S7,S8].

LUMO energy level of $Ru(bpy)_2dppz$ was calculated according to the following equation:[S9]

$$E^* = E - E_{00} / q \quad (12)$$

where E^* is the LUMO energy level and q (=1) is the charge transferred for Ru(III)/Ru(II) couple. E_{00} is energy difference between HOMO and LUMO orbital, calculated through the intersection point of normalized UV spectrum and fluorescent spectrum of $Ru(bpy)_2dppz$ shown in Fig. S17a. E is the redox potential level of Ru(III)/Ru(II) couple at the underground state. The value of E was determined from the cyclic voltamogram shown in Fig. S17b. Please note that the Ag^+/Ag reference electrode was filled with MeCN containing 10 mM $AgNO_3$. Such a reference electrode was calibrated by ferrocenium/ferrocene couple. The difference of its electrode potential from NHE was 0.46 V.

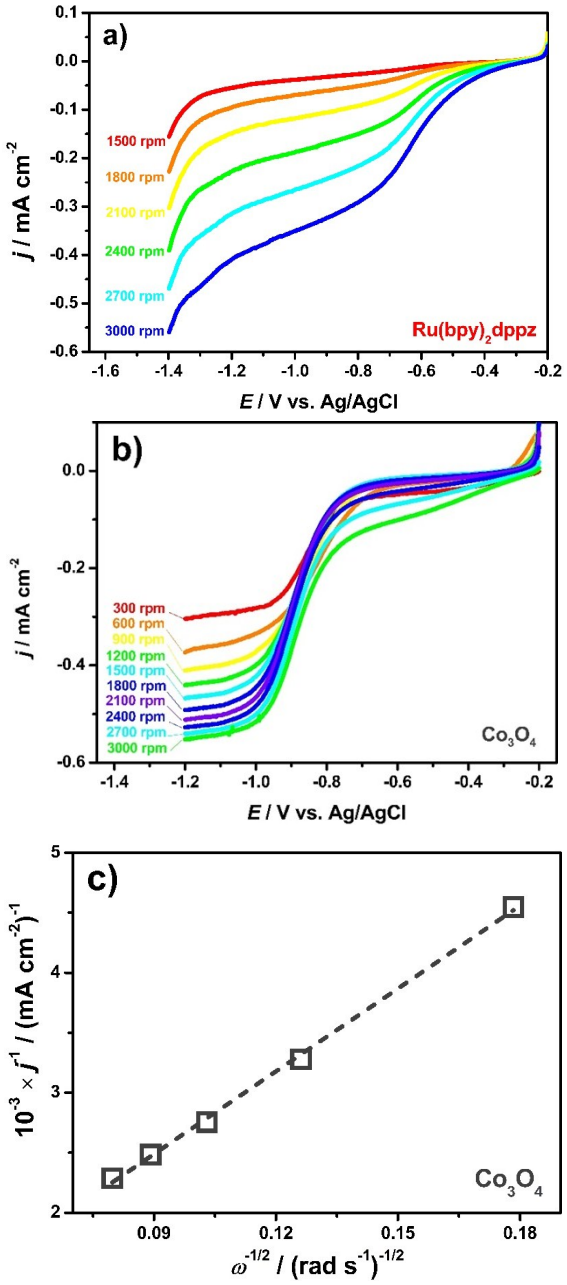

Fig. S18. Hydrodynamic voltammograms of (a) $Ru(bpy)_2dppz$ and (b) Co_3O_4 coated glassy carbon electrode in CO_2 saturated 0.1 M $NaHCO_3$ under various rotation speeds at a scan rate of 5 mV s^{-1}. (c) Koutecky-Levich fitting of (b).

For rotating disk electrode experiments, Koutecky-Levich fitting of the polarization curve was obtained according to Koutecky-Levich equation:[S10]

$$\frac{1}{i} = \frac{1}{i_K} + \frac{1}{0.62nFAD_0^{2/3}\omega^{1/2}\nu^{-1/6}C_0} \tag{13}$$

where i_K is the kinetic current, n is the electron number transferred, F (=96500 C mol^{-1}) is the Faraday constant, D_0 (=1.07×10^{-5} cm s^{-1}) is the diffusion coefficient of CO_2 in 0.1 M $NaHCO_3$, ω is the rotation speed of electrode (in rad s^{-1}), ν (=0.9215 m^2 s^{-1}) is the kinematic viscosity of 0.1 M $NaHCO_3$, C_0 (=0.034 M) is the concentration of CO_2 in 0.1 M $NaHCO_3$.

3. References

[S1] M. F. Wu, Y. N. Jin, G. H. Zhao, M. F. Li, D. M. Li, *Environ. Sci. Technol.* 2010, **44**, 1780.

[S2] G. Sauerbrey, *Z. Phys.* 1959, **155**, 206-222.

[S3] M. D. Koninck, S.-C. Poirier, B. Marsan, *J. Electrochem. Soc*. 2006, **153**, A2103.

[S4] J. Tauc, *Materials Research Bulletin* 1968, **3**, 37-46.

[S5] K. Gelderman, L. Lee, S. W. Donne, *J. Chem. Educ.* 2007, **84**, 685.

[S6] V. Singh, M. Kosa, K. Majhi, D. T. Major, *J. Chem. Theory Comput.* 2015, **11**, 64.

[S7] A. Hagfeldt, G. Boschloo, L. Sun, L. Kloo, H. Pettersson, *Chem. Rev.* 2010, **110**, 6595.

[S8] M. K. Nazeeruddin, A. Kay, I. Rodicio, R. Humphry-Baker, E. Mueller, P. Liska, N. Vlachopoulos, M. Graetzel. *J. Am. Chem. Soc.* 1993, **115**, 6382.

[S9] B.V. Bergeron, G.J. Meyer, *J. Phys. Chem. B* 2003, **107**, 245.

[S10] S. Treimer, A. Tanga, D.C. Johnson, *Electroanalysis* 2002, **14**, 165.